HHS Public Access

Author manuscript

Mol Neurobiol. Author manuscript; available in PMC 2022 June 01.

Published in final edited form as:

Mol Neurobiol. 2021 June ; 58(6): 2574–2589. doi:10.1007/s12035-020-02263-z.

The γ-Protocadherins interact physically and functionally with Neuroligin-2 to negatively regulate inhibitory synapse density and are required for normal social interaction

David M. Steffen[1], **Sarah L. Ferri**[2], **Charles G. Marcucci**[1], **Kelsey L. Blocklinger**[2], **Michael J. Molumby**[1], **Ted Abel**[2], **Joshua A. Weiner**[1,*]

[1]Department of Biology, Iowa Neuroscience Institute, The University of Iowa, Iowa City, IA 52242

[2]Department of Neuroscience and Pharmacology, Carver College of Medicine, Iowa Neuroscience Institute, The University of Iowa, Iowa City, IA 52242

Abstract

Cell adhesion molecules (CAMs) are key players in the formation of neural circuits during development. The γ-protocadherins (γ-Pcdhs), a family of 22 CAMs encoded by the *Pcdhg* gene cluster, are known to play important roles in dendrite arborization, axon targeting, and synapse development. We showed previously that multiple γ-Pcdhs interact physically with the autism-associated CAM Neuroligin-1, and inhibit the latter's ability to promote excitatory synapse maturation. Here, we show that γ-Pcdh can also interact physically with the related Neuroligin-2, and inhibit this CAM's ability to promote inhibitory synapse development. In an artificial synapse assay, γ-Pcdhs co-expressed with Neuroligin-2 in non-neuronal cells reduce inhibitory presynaptic maturation in contacting hippocampal axons. Mice lacking the γ-Pcdhs from the forebrain (including the cortex, the hippocampus, and portions of the amygdala) exhibit increased inhibitory synapse density and increased co-localization of Neuroligin-2 with inhibitory postsynaptic markers *in vivo*. These *Pcdhg* mutants also exhibit defective social affiliation and an anxiety-like phenotype in behavioral assays. Together, these results suggest that γ-Pcdhs negatively regulate Neuroligins to limit synapse density in a manner that is important for normal behavior.

Keywords

synaptogenesis; synapse maturation; cell adhesion; social approach; open field; autism

*Corresponding author: joshua-weiner@uiowa.edu;.

Author's Contributions: D.M.S., S.L.F., M.J.M., T.A., and J.A.W. conceived and planned the experiments; D.M.S, S.L.F., C.G.M., and K.L.B. performed experiments; D.M.S. and S.L.F. analyzed data; D.M.S., S.L.F., and J.A.W. drafted the manuscript; all authors edited the manuscript.

Compliance with ethical standards: The authors have no relevant financial or non-financial interests to disclose, nor any conflicts of interest to declare that are relevant to the content of this article. All authors certify that they have no affiliations with or involvement in any organization or entity with any financial interest or non-financial interest in the subject matter or materials discussed in this manuscript. The authors have no financial or proprietary interests in any material discussed in this article.

Animal Care: All procedures using animals were performed in accordance with The Guide for the Care and Use of Laboratory Animals and were reviewed and approved by the Institutional Animal Care and Use Committee at The University of Iowa.

Consent to Participate: Not applicable; no human subjects.

Consent to Publish: Not applicable; no human subjects.

Introduction

The establishment of functional neural circuits requires multiple orchestrated processes, including axon outgrowth and targeting, dendrite arborization, and synapse formation and maturation. These processes are all regulated by discrete cell-cell contacts between neurons, and between neurons and glial cells, mediated by cell adhesion molecules (CAMs). At these contacts, individual CAM interactions can initiate target recognition, regulate dendrite growth or self-avoidance, promote pre- and post-synaptic differentiation, and facilitate synaptic maturation [1, 2]. The 22 γ-Protocadherins (γ-Pcdhs), cadherin superfamily adhesion molecules encoded by the *Pcdhg* gene cluster, play critical roles during neural development, including promoting neuronal survival [3–7], dendrite arborization [8–10], neurite self-avoidance [11, 12], axon targeting [13, 14], and synapse development [15–20]. The individual γ-Pcdh isoforms (as well as members of the related α-Pcdh and β-Pcdh CAM families encoded by the adjacent *Pcdha* and *Pcdhb* gene clusters) engage in promiscuous *cis* dimerization, but interact strictly homophilically *in trans* [21–27]. The adhesive specificity, diversity, and combinatorial expression of the clustered Pcdh proteins has led to the suggestion that they can provide a molecular code that regulates neural circuit formation [28].

In addition to their *cis*-dimerization and *trans*-homophilic interactions, the γ-Pcdhs have also been reported to interact with other transmembrane molecules. Both α-Pcdhs and γ-Pcdhs have been shown to interact with the receptor tyrosine kinase Ret; this interaction regulates Pcdh phosphorylation and stability as well as turnover of activated Ret [29]. Additionally, one of the 22 γ-Pcdh isoforms, γ-Pcdh-C5, has specifically been shown to interact with the γ2 subunit of the $GABA_A$ receptor, and overexpression of *PcdhgC5* can promote translocation of the $GABA_A$ receptors to the cell surface [18]. We found recently that multiple γ-Pcdh isoforms interact physically and functionally with Neuroligin-1 (Nlg1; [30]), the canonical member of a family of four post-synaptic CAMs (Nlg1–4) that are known to play crucial roles in the maturation and function of synapses [31–37].

Mutations in multiple Nlgs, as well as in their pre-synaptic heterophilic *trans*-interaction partners, the neurexins, are associated with autism spectrum disorder (ASD) and schizophrenia [36, 38, 39], and deficits in social interaction have been observed in some animal models carrying mutations in the Nlgs (reviewed by [40]). Each Nlg preferentially localizes to specific synapse types: Nlg1 at excitatory synapses, Nlg2 and Nlg4 at inhibitory synapses, and Nlg3 at both [41–43]. Through an *in vitro* "artificial synapse assay", in which neurons are co-cultured with heterologous cell lines that are transfected with Nlg or control constructs, Nlgs were shown to promote presynaptic differentiation in contacting axons [35]. Consistent with this, overexpression in neurons leads to increased synapse or spine numbers [44–48], while reducing neuroligin levels decreases synapse or spine numbers [48–50]. Nevertheless, Nlg1/2/3 triple-knockout mice exhibited normal numbers of morphologically-defined synapses; these, however, fail to mature functionally, and triple-knockout mice die at birth, indicating that Nlgs are critical for synaptic maturation [43]. Interestingly, in studies using *in vivo* RNAi-knockdown approaches in a subset of cortical neurons such that Nlg1 levels vary, neurons that lose Nlg1 do exhibit a reduction in synapse density and spinogenesis compared to surrounding control neurons [51]. These discrepancies illustrate

the need to understand the mechanisms through which Nlg function might be regulated between individual neurons in a population.

Recent experiments have indicated new mechanisms that can regulate the synaptogenic and synapse maturation roles of Nlgs. MAM domain containing glycosylphosphatidylinositol (GPI) anchor proteins (MDGA1 and MDGA2) can interact with all Nlgs with differential affinities and can affect synapse formation and function (reviewed by [52]). Both *in vivo* and *in vitro* data demonstrate that MDGA1/Nlg2 interactions negatively regulate inhibitory synapse number and synaptic transmission, while the similar MDGA2 protein negatively regulates excitatory synapse number and synaptic transmission [52–58]. Structural data suggest that MDGA1's immunoglobulin (Ig) domains 1–3 interact with the Nlg2 cholinesterase domain, an extracellular region that overlaps with the Neurexin-binding domain [54]. Similarly, we found that multiple γ-Pcdh isoforms can be co-immunoprecipitated with Nlg1, in an interaction mediated by the extracellular domains of both CAMs [30]. This *cis*-interaction likely disrupts the ability of Nlg1 to efficiently bind its presynaptic partner, neurexin-1β. In the artificial synapse assay, co-expression of a γ-Pcdh isoform in COS cells prevents Nlg1 from promoting presynaptic differentiation; similarly, co-expression of γ-Pcdhs in excitatory neurons disrupts Nlg1's ability to increase dendritic spine density when it is overexpressed [30]. Mice lacking all 22 γ-Pcdhs in the cerebral cortex exhibited significantly *increased* dendritic spine density, confirming that the γ-Pcdhs can negatively regulate synapse development *in vivo.* Together, these studies provide evidence of CAM interactions in *cis* that can negatively regulate the synapse development functions of multiple Nlgs. At least in the case of MDGAs, such CAM interactions can affect behavioral outcomes, including those relevant to neurodevelopmental disorders [53].

In this study, we expand the role of γ-Pcdhs in the regulation of synapse development by identifying their similar negative regulation of Nlg2's ability to promote the development of inhibitory synapses. We show that multiple γ-Pcdh isoforms interact with Nlg2 both *in vitro* and *in vivo via* their extracellular domains, and that both CAMs can co-localize at the cell surface of neurons. Using multiple variations of the artificial synapse assay, we demonstrate that the γ-Pcdhs can attenuate the ability of Nlg2 to promote inhibitory presynaptic differentiation by interacting in *cis* extracellularly. We show that mice lacking γ-Pcdhs in forebrain excitatory neurons (the target of a majority of inhibitory neurons) exhibit a significant increase in cortical inhibitory synapse density and multiple behavioral alterations including deficits in social approach and increased anxiety-like behavior in open-field tests. These results, along with our previous work [30], suggest that γ-Pcdhs act as overall repressors of synapse development in the forebrain through interaction with, and inhibition of, multiple Nlg family members, and are important for the correct development of neuronal circuitry.

Results

Multiple γ-Pcdhs interact with Nlg2 both *in vitro* and *in vivo*

Given our prior demonstration that multiple members of the γ-Pcdh family physically interact with Nlg1 [30], we began this study by asking if γ-Pcdhs might similarly interact with Nlg2. We utilized a co-immunoprecipitation assay in which COS7 (COS) cells were co-

transfected with constructs encoding an N-terminally HA-tagged Nlg2 and either a C-terminally GFP-tagged γ-Pcdh isoform or GFP alone as a negative control. Thirty-six hours after transfection, we lysed the cells, immunoprecipitated the γ-Pcdh protein with anti-GFP antibodies and performed western blots with an anti-HA antibody to detect Nlg2. We were able to co-immunoprecipitate HA-Nlg2 with γ-Pcdh isoform representatives of all three subfamilies (γ-Pcdh-A12, -B1, and -C5), but not with GFP alone (Figure 1A).

Given that this assay involved overexpression of constructs in a heterologous cell line, we sought to confirm the existence of this interaction between endogenous proteins *in vivo*. We prepared whole brain lysates from both adult C57BL/6 wild-type mice and mice homozygous for the *Pcdh-γ*^{fcon3} conditional mutant allele, in which the third constant exon of the *Pcdhg* gene cluster is fused to the coding sequence of GFP, as well as flanked by loxP sites [6]. Thus, all γ-Pcdhs expressed by these mice (prior to Cre excision) contain a GFP tag at their C-terminus (Figure 1C), which we utilized for co-immunoprecipitation by using GFP-Trap beads (Chromo-Tek; GFP nanobody covalently attached to agarose beads), with wild-type lysates serving as a negative control. We were indeed able to co-immunoprecipitate endogenous Nlg2 with GFP-tagged γ-Pcdhs expressed from the endogenous *Pcdhg* cluster in *Pcdh-γ*^{fcon3} mice, suggesting that these two CAMs can interact in the brain *in vivo* (Figure 1B).

Given this evidence that γ-Pcdhs and Nlg2 can interact both *in vitro* and *in vivo*, we sought to identify the γ-Pcdh domains that might participate in this interaction. Each γ-Pcdh comprises an extracellular domain with 6 cadherin (EC) repeats, a transmembrane domain, and a variable cytoplasmic domain, all of which are unique to each isoform, as well as a C-terminal constant domain common to all 22 isoforms (Figure 1C). We co-transfected COS cells with the HA-tagged Nlg2 construct and N-terminally myc-tagged full-length or truncated γ-Pcdh-A3 constructs. The latter included those encoding γ-Pcdh-A3 with a deletion of the cytoplasmic domain (Δcyto), the entire extracellular domain (Δecto), or smaller truncations of EC repeats: Δ1–3, Δ1–4, Δ5–6, or Δ6 only (Figure 1C). Again, after 36 hours of expression, we lysed the cells, immunoprecipitated the tagged γ-Pcdh protein with a myc antibody, and performed western blots using an antibody against the HA-tag on Nlg2. These experiments indicated that Nlg2 co-immunoprecipitated with all γ-Pcdh-A3 deletion constructs tested *except* the one missing the entire extracellular domain (Δecto, Figure 1D). This may indicate that the Nlg2/γ-Pcdh interaction involves multiple EC domains; however, given that the various truncation constructs differ in expression level and efficiency of cell surface delivery in transfected COS cells, we cannot make a firm conclusion. Our data do clearly show that, as was the case for Nlg1 [30], complete, but not partial, loss of the ectodomain abolishes γ-Pcdh interaction with Nlg2.

γ-Pcdh isoforms inhibit the synaptogenic function of Nlg2 in artificial synapse assays

Confirmation of the interaction between the γ-Pcdhs and Nlg2 led us to investigate the functional consequences of this molecular relationship. Armed with previous findings that the γ-Pcdhs can inhibit presynaptic differentiation induced by Nlg1 in the artificial synapse assay [30, 35] we utilized this assay to assess whether the γ-Pcdhs can also attenuate the synaptogenic ability of Nlg2 as well. Dissociated wild-type hippocampal neurons, the axons

of which provided potential “presynaptic sites”, were co-cultured with transfected COS cells, acting as potential “postsynaptic sites”, for 36 hours. The COS cells were transfected with a plasmid encoding HA-tagged Nlg2 along with those encoding either a myc-tagged γ-Pcdh isoform (γ-Pcdh-A3 or -C3) or RFP-tagged CD4 as a negative control; COS cells expressing only CD4-RFP, which is not synaptogenic in this assay [30, 58] served as a baseline control. Presynaptic differentiation was identified by staining with antibodies for synapsin, a universal presynaptic marker, and measuring its signal intensity in axons contacting individual COS cells, normalized to COS cell area. Efficient expression of the transfected CAMs was confirmed through immunostaining for the HA and myc tags or through RFP fluorescence (Figure 2A). As expected, Nlg2 expression in COS cells significantly increased presynaptic differentiation in contacting axons compared to the baseline control (Figure 2B). This increase in presynaptic differentiation was significantly attenuated when either γ-Pcdh isoform, but not CD4, was co-expressed with Nlg2 (Figure 2B). As we showed previously for Nlg1 [30], this inhibitory effect of γ-Pcdh co-expression was not due to a reduction in the overall levels of Nlg2 (Figure 2C) nor in surface expression of Nlg2 (Figure 2D) We conclude that the γ-Pcdhs are capable of inhibiting the synaptogenic ability of Nlg2 in the artificial synapse assay, as previously we showed they could for Nlg1 [30].

Given that co-immunoprecipitation data indicate that γ-Pcdh proteins interact with Nlg2 extracellularly (Figure 1), we ascertained the extent to which functional inhibition of Nlg2 depends on the ectodomain. We repeated the artificial synapse assay, this time transfecting COS cells with HA-tagged Nlg2 and myc-tagged γ-Pcdh-A3 FL, ΔEcto, or ΔCyto constructs (Figure 1C) or the CD4 negative control (Figure 3A). As expected, full-length γ-Pcdh-A3 significantly inhibited Nlg2’s ability to induce pre-synaptic differentiation, as did A3Δctyo (Figure 3A,B). In contrast, A3ΔEcto expression had no effect on Nlg2 induction of presynaptic differentiation (Figure 3A,B). One caveat here is that cell surface delivery of the A3ΔEcto construct, while observable, did not appear to be as efficient as that of A3FL or of A3Δctyo, consistent with prior results [26]. Nevertheless, these results, in conjunction with co-immunoprecipitation experiments (Figure 1) are consistent with the γ-Pcdhs mediating inhibition of Nlg2 function through extracellular interactions.

We also analyzed this set of artificial synapse assays multiple ways to determine more precisely how γ-Pcdh-A3 affected Nlg2’s promotion of pre-synaptic differentiation. In the standard assay (Figure 2), total intensity of synapsin immunostaining over the COS cell surface is taken as a measure of the synaptogenic effect. Co-expression of γ-Pcdhs could reduce this measure by lowering the number of synapsin puncta, or by reducing the intensity of each synapsin punctum. We found support for the former possibility: While we found no significant difference in the fluorescence intensity of individual pre-synaptic puncta across COS cell transfection conditions (Figure 3D), we did find that the number of synapsin puncta per COS cell was significantly decreased in COS cells co-expressing A3FL and A3ΔCyto, but not in those co-expressing A3ΔEcto (Figure 3C). We also immunostained these co-cultures with the TUJ1 antibody that recognizes neuron-specific tubulin, and found that a similar density of neurites grew over COS cells regardless of transfection condition (Figure 3E). Together, these data indicate that the γ-Pcdhs interact with Nlg2 extracellularly via their ectodomains to prevent the formation of pre-synaptic puncta in contacting axons.

Although Nlg2 is preferentially localized to GABAergic synapses [43], when overexpressed it can promote the differentiation of both excitatory and inhibitory presynaptic sites *via* interactions with neurexins [45, 59]. The standard artificial synapse assay described above uses clustering of synapsin, a vesicle protein present at both excitatory and inhibitory presynaptic sites, and the majority of neurons in hippocampal cultures are excitatory, with perhaps only 10–15% inhibitory interneurons. We thus next sought to modify the assay to focus on inhibitory presynaptic sites. We cultured hippocampal neurons from a mouse strain expressing GFP from the glutamic acid decarboxylase 67 (GAD67) promoter [60, 61], which allowed us to highlight the small percentage of inhibitory interneurons in our co-cultures. For this assay, COS cells were transfected with a construct encoding HA-tagged Nlg2 either by itself or with a plasmid encoding a myc-tagged γ-Pcdh isoform (A3 or C3) (Figure 4A). We utilized the GFP signal to identify fields in which inhibitory interneurons contacted COS cells and quantified the fluorescence intensity of their presynaptic terminals (normalized to COS cell area), immunostained with an antibody against the vesicular GABA transporter (VGAT). The intensity of VGAT+ presynaptic clustering was significantly reduced when a γ-Pcdh construct was co-expressed with Nlg2 compared to when Nlg2 was expressed alone (Figure 4B), confirming that that the γ-Pcdhs can attenuate the ability of Nlg2 to induce inhibitory presynaptic differentiation in axons.

γ-Pcdhs can be co-aggregated with Nlg2 on the neuronal cell surface

We previously reported that γ-Pcdhs can interact in *cis* with Nlg1 at the neuronal cell surface [30]; we thus next asked if such *cis* interactions also occur with Nlg2 in neurons. To investigate this, we sparsely lipofected hippocampal neurons at 9 days in vitro (9 DIV) with constructs encoding GFP (to reveal neuronal morphology), HA-Nlg2, and either myc-A3, myc-C3, or CD4-RFP. On 12 DIV, we artificially aggregated Nlg2 on the surface of neurons through the addition to the cell-culture media of anti-HA antibodies for 30 minutes, following which the media was changed to that containing the appropriate secondary antibody. After another 30 minutes, the media was changed again, and neurons cultured for an additional 16 hours (Figure 5A; methods adapted from [30, 58]). We observed that both γ-Pcdhs tested (A3 and C3) but not the control protein (CD4), co-aggregated in *cis* with HA-Nlg2 both on dendritic segments (Figure 5B) and on neuronal somas (Figure 5C), providing evidence that the interaction between these two CAMs that we observed in co-immunoprecipitations (Figure 1) and inferred from artificial synapse assays (Figure 3) can also occur on neuronal cell surfaces.

Mice lacking γ-Pcdhs show increased inhibitory synapse puncta density and more synaptic Nlg2

We previously showed that *Pcdhg* null cortical excitatory neurons exhibited a significant increase in dendritic spine density and excitatory synaptic puncta, consistent with the ability of γ-Pcdh proteins to inhibit Nlg1 in *in vitro* artificial synapse assays and in cultured neurons [30]. If the γ-Pcdhs can inhibit Nlg2's ability to promote the maturation of inhibitory synapses by interacting with it in *cis*, we reasoned that loss of γ-Pcdhs from excitatory neurons might result in an overall higher density of synapses made on them by inhibitory interneurons *in vivo.* To test this, we utilized a compound transgenic mouse (*Emx1-Cre;Pcdhg*$^{fcon3/fcon3}$; previously described [8, 9] in which all γ-Pcdhs are absent

from excitatory neurons (as well as astrocytes) of the dorsal forebrain, including the cerebral cortex, hippocampus, and portions of the basolateral amygdala [62]. We stained cryosections for inhibitory synaptic markers VGAT (pre-synaptic) and gephyrin (post-synaptic) and estimated the density of inhibitory synapses by counting the number of overlapping immunoreactive puncta from multiple single plane confocal images within layer V of primary somatosensory cortex (Figure 6A). Indeed, we found a significant increase in the number of gephyrin puncta, and in the number of overlapping pre- and post-synaptic puncta, in mutants compared to controls (Figure 6B–D); VGAT puncta showed no significant difference.

Based on the *in vitro* results from the artificial synapse assays (Figures 2–4), and on our prior published work [30] we hypothesized that γ-Pcdhs might regulate inhibitory synapse development through relocating Nlg2 peri-synaptically. Though we have found no evidence that γ-Pcdhs remove Nlg1 [30] or Nlg2 (Figure 2) from the surface of cells, it is possible that interactions between the often peri-synaptic γ-Pcdhs [15, 63] and Nlgs could sequester the latter away from the synapse. We stained cryosections of 5–6 week old *Emx1-Cre;Pcdhg*$^{fcon3/fcon3}$ and control cortex for both Nlg2 and gephyrin to investigate any differences in the density of Nlg2+ post-synaptic puncta (Figure 7A). We found that in the absence of γ-Pcdhs, the proportion of Nlg2 that colocalized with gephyrin increased significantly (Figure 7B), and there was also a similar increase in the total area of Nlg2+/gephyrin+ colocalized puncta (Figure 7C.) Though other interpretations are possible, these data are consistent with the possibility that γ-Pcdhs negatively regulate inhibitory synapse development by localizing Nlg2 away from post-synaptic sites.

Pcdhg forebrain mutants exhibit behavioral defects

Behavioral disruptions consistent with those seen in ASD, such as reduced social affiliation and increased anxiety, have been associated with altered expression of many synaptic CAMs, including some neuroligins and protocadherins [40, 64] Given the increased density of both excitatory [30] and inhibitory (this study) synapses in the absence of γ-Pcdhs, we asked whether forebrain-restricted *Pcdhg* mutants might exhibit alterations in ASD-relevant behaviors. We tested male and female *Emx1-Cre;Pcdhg*$^{fcon3/fcon3}$ (KO) and *Emx1-Cre;Pcdhg*$^{fcon3/+}$ (Het) control mice in social approach, open field, and contextual fear conditioning tests. For the three-chamber social approach test, we measured the amount of time spent sniffing each of two cylinders over two separate phases, as well as total distance traveled. In Phase 1, both cylinders were empty, while in Phase 2, one cylinder contained a novel object (nonsocial cylinder) and the other a novel mouse (social cylinder). To focus on social affiliative behavior and reduce potential sexual and aggressive motivations of the test mouse, we used a same-sex, gonadectomized mouse of a docile strain, A/J, as the social stimulus. We used a repeated measures two-way ANOVA to test main effects of genotype, phase, and the genotype x phase interaction. In Phase 1, there was no difference between *Pcdhg* mutants and control littermates in distance traveled (Figure 8A). In Phase 2, however, mutant mice traveled significantly less than did controls ($p<0.01$; Figure 8B). Time spent sniffing the nonsocial cylinder in Phase 1, when it was empty, was similar to that in Phase 2, when it contained a novel object, for both genotypes (Figure 8C). For social sniffing, however, *Pcdhg* mutants spent a similar amount of time sniffing the social cylinder in Phase

1 when it was empty as controls, but significantly less time sniffing the social cylinder than controls in Phase 2 when it contained the novel social stimulus mouse (Figure 8D), indicating social approach deficits in the absence of cortical γ-Pcdhs. In the open field test, *Pcdhg* mutants spent significantly less time in the center than did littermate controls (Figure 8F), despite not differing in total distance traveled (Figure 8E). This indicates that in the absence of cortical γ-Pcdhs, mice exhibit an anxiety-like phenotype. However, *Pcdhg* mutants performed similarly to control mice in contextual fear conditioning (Figure 8G), indicating that hippocampus-dependent fear memory remains intact despite loss of all γ-Pcdhs in excitatory neurons there.

Discussion

Exquisitely regulated formation of excitatory and inhibitory synapses is critical for the establishment of functional neuronal circuits. Discrepancies in the balance of excitatory and inhibitory inputs are thought to play a role in many human diseases including epilepsy, schizophrenia, and ASD [65, 66]. We previously presented evidence that γ-Pcdhs act as negative regulators of excitatory synapse formation in the cerebral cortex, and identified their interaction with, and inhibition of, Nlg1 as a possible mechanism [30]. Here we present evidence that: 1) multiple γ-Pcdh isoforms can also bind to Nlg2 *via* their extracellular domains, both *in vitro* (in transfected cell lines and on the surface of neurons) and *in vivo* (in brain lysates); 2) multiple γ-Pcdhs can attenuate the ability of Nlg2 to promote inhibitory presynaptic differentiation in artificial synapse assays *in vitro* via extracellular domain interactions; 3) loss of the γ-Pcdhs from excitatory neurons of the forebrain *in vivo* (the postsynaptic sites of many inhibitory neurons) results in increases in the density of inhibitory synaptic puncta and in the proportion of post-synaptically-localized Nlg2; and 4) behaviorally, *Pcdhg* mutants exhibit an anxiety-like phenotype and deficits in social approach. Together, these data suggest conserved functionality within the γ-Pcdh family to negatively regulate both excitatory and inhibitory synapse development through interactions with multiple neuroligin family members, which plays a role in proper neural circuit development.

As we found previously for the interaction with Nlg1 [30], we show that γ-Pcdhs interact with Nlg2 *via* their extracellular domains. Also as before [30], γ-Pcdhs in our experiments preferentially co-immunoprecipitated the lower of the two Nlg2 bands (likely an immaturely glycosylated form) in transfected cell lines, but the upper of the two Nlg2 bands (likely the mature glycosylated form [67, 68]) in the brain *in vivo* (Figure 1). In each case, the band preferentially pulled down was the more abundant form, so this may simply represent a detection-limit issue. We find that deletion of various combinations of individual γ-Pcdh EC domains (e.g., ΔEC1–3, ΔEC6) did not completely disrupt our ability to co-immunoprecipitate them with Nlg2 (Figure 1), though the efficiency of pulldown did appear to vary. Given the caveat that these experiments necessitated using overexpression of tagged constructs in heterologous cells, we can only conclude, tentatively, that γ-Pcdh interactions with Nlg2 (and with Nlg1; [30]) are mediated by redundant interactions involving multiple EC domains. Though we have not addressed whether γ-Pcdhs interact directly with Nlg2, in our prior work we did find this to be the case for their interactions with Nlg1 [30]. Recently, the structures of γ-Pcdhs (and their clustered Pcdh brethren, the α- and β-Pcdh proteins) and

the mechanisms of their homophilic interaction have been intensively studied. Our prior biochemical experiments had indicated the importance of EC2 and EC3 in regulating the specificity of γ-Pcdh *trans* interactions [26], and structural data are consistent with this, showing extensive antiparallel interactions involving EC1-EC4 [22, 24, 25, 69]. These antiparallel *trans* interactions, coupled with *cis* dimerization *via* EC5 and EC6, result in a multimeric lattice of γ-Pcdh dimers between two cell membranes sharing the same isoform expression pattern [70].

Given this, how might we envision heterophilic *cis*-interactions, such as those we've shown with Nlgs or those reported with the receptor tyrosine kinase Ret [29] or the γ2 subunit of the $GABA_A$ receptor [18]? We suggest that one possibility is that these heterophilic *cis*-interactions involve γ-Pcdh isoforms that do not match those expressed by contacting cells, and that are thus excluded from the homophilic *trans*-lattice structure. If this is the case, then "mis-matched" γ-Pcdhs in a given cell could still subserve important functions outside of homophilic interactions; as the lattice structure is broken up by mismatches (as predicted by [25, 27]), γ-Pcdh function might switch from cell-cell interaction to signaling roles. As noted above, another adhesion protein, MDGA1, can negatively regulate the *in vitro* synaptogenic activity of Nlg2 [57, 58]. Recent structural studies have shown that MDGA1's Ig1–3 domains interact with dimers of Nlg2. MDGA1 interactions occur in the same domain of Nlg2 that interacts with neurexin, indicating that MDGA1 competes with neurexin for Nlg2 binding [54–56]. In our prior work [30], we showed that co-expression of γ-Pcdhs with Nlg1 in cells disrupts surface binding of soluble neurexin, and given the similar co-immunoprecipitation results this is almost certainly the case for Nlg2 as well. It would be helpful if future structural studies were able to crystalize Nlgs or other interacting proteins along with γ-Pcdhs in order to address this possibility.

The results from our *in vivo* experiments show that the total number of inhibitory synaptic puncta was increased in mice which lack γ-Pcdhs, consistent with a generally negative regulation of inhibitory synapse density by γ-Pcdhs. These results parallel those we reported previously: dendritic spines were also more plentiful in *Pcdhg* forebrain mutants, though the proportion of spines that exhibited a mature mushroom morphology was reduced [30]. We hypothesize that in the absence of γ-Pcdhs, both Nlg1 and Nlg2 are either more "active" (e.g., more free to bind to presynaptic neurexin) or are better localized to the synapse (many γ-Pcdhs localize peri- or extra-synaptically, so in binding Nlgs they could alter their synaptic localization), resulting in an increase in the validation or maturation of nascent synaptic contacts. We found evidence for the latter possibility here (Figure 7). While *in vitro* artificial synapse assays clearly indicate that γ-Pcdhs can inhibit the ability of Nlg1 and Nlg2 to promote presynaptic differentiation, we cannot yet conclude that the synaptic phenotypes in *Pcdhg* forebrain mutants are due directly to heightened Nlg function. For test this, *Pcdhg* mutants could be bred to Nlg mutant mouse lines (which generally do not exhibit altered synapse density; [37]), to see if synapse density is still increased upon γ-Pcdh loss even when Nlgs are absent. However, given that all 4 Nlgs can exhibit overlapping functions, this would require compound mice (double, triple or quadruple Nlg mutation plus conditional loss of γ-Pcdhs) with more alleles than would be practical. An alternative approach would be that utilized by [51], in which Nlg1 was knocked down using shRNA in scattered cortical neurons, which did result in reduced spine density and spinogenesis,

apparently due to a mismatch in Nlg levels between neurons; such experiments in *Pcdhg* forebrain mutants, however, might be difficult to interpret given the opposing effects on synapse density of γ-Pcdh loss and Nlg knockdown. In any case, our results here and in [30] are consistent with the findings of Chanda, et al. [71], who performed many careful experiments that together indicate that Nlgs do not contribute to initial synapse formation, but rather promote the maturation of the post-synaptic machinery. Interactions of Nlgs with *cis*-transmembrane partners such as the γ-Pcdhs or MDGAs likely provides a kind of "brake" on their ability to validate or mature synapses, adding another layer of regulation that helps establish proper synapse density.

Here we also find that mice lacking the γ-Pcdhs in the forebrain exhibit an anxiety-like phenotype in the open field test, and deficits in social approach in a three-chamber test. These *Pcdhg* forebrain mutants exhibit not only the increased inhibitory synaptic puncta shown here, but also an increase in total dendritic spine density (many of them immature thin spines) and excitatory synaptic puncta [30]; we cannot yet address the extent to which altered inhibitory vs. excitatory synapse density might contribute to these behavioral phenotypes. A number of CAMs have been linked to neurodevelopmental disorders, including ASD, and several mouse models involving cadherins and protocadherins have demonstrated similar deficits as presented here [40, 64, 72, 73]. In addition, many prior studies [40] have assessed social affiliation behaviors in many lines of mice in which Nlgs are deleted (constitutively or conditionally), overexpressed, or disrupted by ASD-associated point mutations. Knockout or knockdown of Nlg2 generally had no or little reported effect on social affiliation behaviors [74–77]; in contrast, widespread overexpression of Nlg2 did decrease social interaction and social preference [47]. Given that these *Pcdhg* conditional mutants exhibit severely reduced dendrite arborization and dysregulation of a FAK/PKC/MARCKS pathway [8] important for normal neuronal function, we can't yet conclude that the behavioral defects we report here are attributable to the enhanced Nlg2 function we hypothesize; nevertheless, it is intriguing that our behavioral results are congruent with those reported for Nlg2 over-expressing mice [47].

Methods

Mouse strains.

All animals and associated procedures were approved by the University of Iowa's institutional animal care and performed in compliance with NIH guidelines for the use of animals. In all experiments using hippocampal neurons, mice were dissected at postnatal day 0. Hippocampal neurons were dissected from C57/BL6J wild-type mice for the non-specific (synapsin-stained) artificial synapse assay. For the inhibitory-specific (VGAT-stained) artificial synapse assay, CD1 mice heterozygous for knock-in allele expressing green fluorescent protein (GFP) from the endogenous glutamic acid decarboxylase-67 (GAD67) promoter [61] were utilized; these were the kind gift of Dr. Hanna Stevens, University of Iowa Department of Psychiatry and Iowa Neuroscience Institute. For the *in vivo* co-IP, brain lysates were prepared from C57/BL6J wild-type mice and transgenic mice of the *Pcdh-γ*^{fcon3} strain, congenic on C57/BL6J (described by [6]). For *in vivo* inhibitory post-synaptic density, and inhibitory synapse counts, *Emx1-Cre* line (Stock #005628, obtained from The

Jackson Laboratory; [62]) were used as control animals and *Pcdh-γ* ^{fcon3} mice were bred with the Emx1-Cre line to generate forebrain conditional knock-outs. The *Emx1-Cre* line is active in excitatory neurons and astrocytes of the cortex and hippocampus as well as some neurons of the basolateral amygdala [62].

Antibodies.

The following primary antibodies were used: rat, anti-HA (Roche); rabbit, anti-Myc (Cell Signaling Technologies); rabbit anti-DsRed (Takara 632496); rabbit anti-Synapsin 1 (Invitrogen A6442); rabbit anti-Neuroligin-2 (Synaptic Systems 129203) rabbit anti-VGAT (Chemicon AB5855); mouse anti-GFP (Molecular Probes A11120) mouse anti-Gephyrin (Synaptic Systems 147 011); mouse anti-HA (Roche 11 583 816); rabbit anti-synapsin-1XP (Cell Signaling); guinea pig anti-VGAT (Chemicon); Chicken anti-GFP (Invitrogen A10262). Animal-specific fluorescently-tagged secondary antibodies from Invitrogen were used. HRP-tagged secondaries for western blots: anti-mouse (Pierce 31430), anti-rabbit (Jackson ImmunoResearch 111-035-003). The mouse anti-Myc-9E10 monoclonal antibody was obtained from the Developmental Studies Hybridoma Bank, created by the NICHD of the NIH and maintained at The University of Iowa, Department of Biology, Iowa City, IA 52242.

Plasmids.

All γ-Pcdh (GFP-tagged and myc-Tagged) and HA-Nlg2 plasmids used in both co-IP studies and artificial synapse assays are derived from the mouse protein sequence and were described previously [26, 30].

In vitro co-IP assays.

Plasmids used for transfections included: an N-terminally HA-tagged Nlg2 construct, N-terminally myc-tagged γ-Pcdh-A3 deletion constructs, and C-terminally GFP-tagged γ-Pcdh full-length constructs. COS7 cells were co-transfected using Lipofectamine 2000 in 6 cm dishes with the indicated constructs and incubated with 2.5 ml of growth media. After 36–48 hours of expression, cells were collected in cold phosphate-buffered saline (PBS) via scraping and centrifuged at 12,000 X g for 10 min to clear cell debris. Two micrograms of rabbit anti-myc (Cell Signaling Technologies) were added to 0.5 ml of lysate and incubated on a rotator overnight at 4°C. The following day, protein-A/G agarose beads, or protein-G magnetic Dynabeads (ThermoFisher), were added and incubated for an additional 3 hours at 4°C on a rotator. Next, beads were washed four times with lysis buffer, resuspended in Laemmli buffer, and analyzed by SDS/PAGE and western blot. All co-immunoprecipitation assays were performed using multiple biological (distinct animals or distinct cell culture transfections) and technical (distinct immunoprecipitation tubes, gels, and blots from each biological sample) replicates.

Hippocampal neuronal cultures and artificial synapse assay.

Wild-type and transgenic neuronal cultures were generated from pooled hippocampal tissue from either P0 C57BL/6J or CD1/GAD67 pups (described above). Hippocampal cultures were plated onto 18-mm German glass coverslips (coated with Matrigel [Corning] diluted

1:50 in Neurobasal media) at a density of 100,000 cells per coverslip, and were maintained in Neurobasal supplemented with GlutaMAX, B27 or GS21 supplements (Invitrogen), and penicillin/streptomycin. For artificial synapse assays, at 8 DIV, each coverslip of neurons was incubated with 60,000 co-transfected COS7 cells and co-cultures were fixed and analyzed after a further 36 hours [78]. COS7 cells were obtained from ATCC and utilized at low passage numbers.

Co-aggregation Assay.

Hippocampal neurons were transfected after 9 DIV as specified previously. At 12 DIV, neurons were incubated with rat anti-HA (Roche 3F10) for 30 min, then transferred into media containing Alexa 647 Donkey anti-Rat (Jackson Labs). After 30 min incubation in secondary antibodies, neurons were transferred back into conditioned media supplemented with fresh Neurobasal for 16 hours before being fixed, washed, and stained for proteins of interest. Co-aggregation studies were performed using multiple biological and technical replicates.

Brain lysate & *in vivo* co-IP.

Whole brains were dissected from both adult C57 wild-type mice and adult C57 homozygous transgenic mice of the *Pcdhg*^{fcon3} strain, in which all γ-Pcdh proteins are tagged at the C-terminus with GFP. Tissue was homogenized in mild lysis buffer (50 mM, pH 7.4, 150 mM NaCl, 1% Triton X-100, 25 mM NaF, plus protease inhibitor [Roche mini Complete]), incubated on ice for 5 minutes, and then cleared by centrifugation at 10,000 x g for 15 min at 4°C. The lysate's protein content was analyzed using the Pierce® BCA Protein Assay in order to collect 300 μg of protein. Chromotek's GFP-Trap® beads were equilibrated in mild lysis buffer and pelleted by centrifugation at 2,500 x g for 2 minutes at 4°C. Collected lysate was added to equilibrated GFP-Trap® beads, incubated on a rotator for 1 hour at 4°C, and beads were pelleted by centrifugation. Beads were washed three times with mild lysis buffer, pelleted by centrifugation, resuspended in 100 ml of 2x Laemmli buffer, and boiled for 10 min at 95°C. Samples were analyzed by SDS/PAGE and western blot.

Image collection.

Images were collected using a Lecia Sp2 ABOS laser-scanning confocal microscope. Z-stacks of 0.5 micron step-sizes were taken for co-aggregation and artificial synapse assays using a 20x objective. For artificial synapse assays, co-transfected COS7 cells in neurite-dense areas were selected for imaging at random, without examination of the synapsin or VGAT signal. COS7 cell boundaries were outlined in FIJI, all synapsin or VGAT signal within the area of the cell was isolated by thresholding, and the integrated density was quantified relative to COS7 cell area. Additionally, HA-Nlg2 average integrated density was quantified relative to cell area to ensure there were no significant HA-Nlg2 expression differences between conditions. *In vivo* cortical confocal single-plane images were taken using 63x objective. All images shown were chosen to be representative of the average data for each experiment and condition.

Social Approach Test.

The Social Approach Test (SAT) procedure was conducted as previously described [79–81] in juvenile mice, aged 28–32 days old. A top- and bottom-less three-chambered black Plexiglas arena (10 × 20.5 × 9 in) was placed on clean bench paper on a clear Plexiglass stand lit from underneath by infrared lights. End chambers contained a transparent Plexiglas cylinder with holes for air circulation and olfactory exploration. Experiments were conducted under dim lighting in order to encourage exploration and decrease anxiety-related behavior. Sessions were recorded and analyzed with a Basler Ace IR camera and Ethovision software (Noldus).

For Phase 1, a test mouse was placed in the apparatus and was allowed to explore for 10 minutes. In Phase 2 a gonadectomized, same-sex A/J mouse (social stimulus) was placed in one cylinder (the social cylinder) and a novel object (large plastic Lego block) into the other cylinder (the nonsocial cylinder) and the test mouse was allowed to move freely throughout the apparatus for 10 minutes. Distance traveled and amount of time spent sniffing were quantified. Experimenters were blinded to genotype during testing and analysis. n= 11 mice for control condition and n= 15 mice for the KO condition.

Open Field.

Mice from the SAT were subjected to open field testing at 60–90 days old. After 30 min acclimation to the room, mice were placed in a brightly lit open field measuring 12” x 12” x 16” for 6 minutes. Sessions were recorded and analyzed with a Basler Ace camera and Ethovision software (Noldus). Distance traveled and time spent in center versus periphery (50% of area) were quantified. Experimenters were blinded to genotype during testing and analysis. n=9 mice for the control condition and n=19 mice for the KO condition.

Contextual Fear Conditioning.

At 90–110 days old, mice were tested for contextual fear conditioning. Mice were placed in an electrified grid floor chamber inside a sound attenuated box for 3 min. After 2.5 min of free exploration, a 2-second, 1.5 mA footshock was delivered. The mice were removed after an additional 30 s. Twenty-four hours later mice were placed in the same chamber for 5 min. Freezing was measured continuously by FreezeScan software (CleverSys Inc). Experimenters were blinded to genotype during testing and analysis. n=10 mice for the control condition and n=16 mice for the KO condition.

Statistical Analysis.

Analyses were performed using Prism (Graph Pad software). Comparisons between conditions were made using one-way ANOVA, with Tukey’s multiple comparisons test. For behavioral tests, GraphPad Prism was used to conduct repeated measures two-way ANOVA with Bonferroni’s post-hoc test where appropriate or Student’s t-test. The threshold for significance was $p<0.05$.

Acknowledgements:

We thank Leah Fuller for expert assistance with mouse colony management and members of the Weiner laboratory for helpful comments. We are grateful to Dr. Hanna Stevens, University of Iowa Department of Psychiatry and Iowa Neuroscience Institute, for sharing the GAD67-GFP mouse line.

Funding: This work was supported by NIH R01 NS055272 to J.A.W. S.L.F. is supported by NIH K01 MH119540. Work in the laboratory of T.A. is supported by the Carver College of Medicine and the Roy J. Carver Chair in Neuroscience.

References

1. de Wit J and Ghosh A, Specification of synaptic connectivity by cell surface interactions. Nat Rev Neurosci, 2016. 17(1): p. 22–35. [PubMed: 26656254]
2. Missler M, Sudhof TC, and Biederer T, Synaptic cell adhesion. Cold Spring Harb Perspect Biol, 2012. 4(4): p. a005694. [PubMed: 22278667]
3. Garrett AM, et al., CRISPR/Cas9 interrogation of the mouse Pcdhg gene cluster reveals a crucial isoform-specific role for Pcdhgc4. PLoS Genet, 2019. 15(12): p. e1008554. [PubMed: 31877124]
4. Ing-Esteves S, et al., Combinatorial Effects of Alpha- and Gamma-Protocadherins on Neuronal Survival and Dendritic Self-Avoidance. J Neurosci, 2018. 38(11): p. 2713–2729. [PubMed: 29439167]
5. Lefebvre JL, et al., gamma-Protocadherins regulate neuronal survival but are dispensable for circuit formation in retina. Development, 2008. 135(24): p. 4141–51. [PubMed: 19029044]
6. Prasad T, et al., A differential developmental pattern of spinal interneuron apoptosis during synaptogenesis: insights from genetic analyses of the protocadherin-gamma gene cluster. Development, 2008. 135(24): p. 4153–64. [PubMed: 19029045]
7. Wang X, et al., Gamma protocadherins are required for survival of spinal interneurons. Neuron, 2002. 36(5): p. 843–54. [PubMed: 12467588]
8. Garrett AM, et al., gamma-protocadherins control cortical dendrite arborization by regulating the activity of a FAK/PKC/MARCKS signaling pathway. Neuron, 2012. 74(2): p. 269–76. [PubMed: 22542181]
9. Molumby MJ, Keeler AB, and Weiner JA, Homophilic Protocadherin Cell-Cell Interactions Promote Dendrite Complexity. Cell Rep, 2016. 15(5): p. 1037–1050. [PubMed: 27117416]
10. Suo L, et al., Protocadherin clusters and cell adhesion kinase regulate dendrite complexity through Rho GTPase. J Mol Cell Biol, 2012. 4(6): p. 362–76. [PubMed: 22730554]
11. Lefebvre JL, Neuronal territory formation by the atypical cadherins and clustered protocadherins. Semin Cell Dev Biol, 2017. 69: p. 111–121. [PubMed: 28756270]
12. Lefebvre JL, et al., Protocadherins mediate dendritic self-avoidance in the mammalian nervous system. Nature, 2012. 488(7412): p. 517–21. [PubMed: 22842903]
13. Hasegawa S, et al., Clustered Protocadherins Are Required for Building Functional Neural Circuits. Front Mol Neurosci, 2017. 10: p. 114. [PubMed: 28484370]
14. Prasad T and Weiner JA, Direct and Indirect Regulation of Spinal Cord Ia Afferent Terminal Formation by the gamma-Protocadherins. Front Mol Neurosci, 2011. 4: p. 54. [PubMed: 22275881]
15. Garrett AM and Weiner JA, Control of CNS synapse development by {gamma}-protocadherin-mediated astrocyte-neuron contact. J Neurosci, 2009. 29(38): p. 11723–31. [PubMed: 19776259]
16. Keeler AB, Molumby MJ, and Weiner JA, Protocadherins branch out: Multiple roles in dendrite development. Cell Adh Migr, 2015. 9(3): p. 214–26. [PubMed: 25869446]
17. Kostadinov D and Sanes JR, Protocadherin-dependent dendritic self-avoidance regulates neural connectivity and circuit function. Elife, 2015. 4.
18. Li Y, et al., Molecular and functional interaction between protocadherin-gammaC5 and GABAA receptors. J Neurosci, 2012. 32(34): p. 11780–97. [PubMed: 22915120]
19. Peek SL, Mah KM, and Weiner JA, Regulation of neural circuit formation by protocadherins. Cell Mol Life Sci, 2017. 74(22): p. 4133–4157. [PubMed: 28631008]

20. Weiner JA, et al., Gamma protocadherins are required for synaptic development in the spinal cord. Proc Natl Acad Sci U S A, 2005. 102(1): p. 8–14. [PubMed: 15574493]
21. Goodman KM, et al., Protocadherin cis-dimer architecture and recognition unit diversity. Proc Natl Acad Sci U S A, 2017. 114(46): p. E9829–E9837. [PubMed: 29087338]
22. Goodman KM, et al., gamma-Protocadherin structural diversity and functional implications. Elife, 2016. 5.
23. Nicoludis JM and Gaudet R, Applications of sequence coevolution in membrane protein biochemistry. Biochim Biophys Acta Biomembr, 2018. 1860(4): p. 895–908. [PubMed: 28993150]
24. Nicoludis JM, et al., Structure and Sequence Analyses of Clustered Protocadherins Reveal Antiparallel Interactions that Mediate Homophilic Specificity. Structure, 2015. 23(11): p. 2087–98. [PubMed: 26481813]
25. Rubinstein R, et al., Molecular logic of neuronal self-recognition through protocadherin domain interactions. Cell, 2015. 163(3): p. 629–42. [PubMed: 26478182]
26. Schreiner D and Weiner JA, Combinatorial homophilic interaction between gamma-protocadherin multimers greatly expands the molecular diversity of cell adhesion. Proc Natl Acad Sci U S A, 2010. 107(33): p. 14893–8. [PubMed: 20679223]
27. Thu CA, et al., Single-cell identity generated by combinatorial homophilic interactions between alpha, beta, and gamma protocadherins. Cell, 2014. 158(5): p. 1045–1059. [PubMed: 25171406]
28. Yagi T, Molecular codes for neuronal individuality and cell assembly in the brain. Front Mol Neurosci, 2012. 5: p. 45. [PubMed: 22518100]
29. Schalm SS, et al., Phosphorylation of protocadherin proteins by the receptor tyrosine kinase Ret. Proc Natl Acad Sci U S A, 2010. 107(31): p. 13894–9. [PubMed: 20616001]
30. Molumby MJ, et al., gamma-Protocadherins Interact with Neuroligin-1 and Negatively Regulate Dendritic Spine Morphogenesis. Cell Rep, 2017. 18(11): p. 2702–2714. [PubMed: 28297673]
31. Craig AM and Kang Y, Neurexin-neuroligin signaling in synapse development. Curr Opin Neurobiol, 2007. 17(1): p. 43–52. [PubMed: 17275284]
32. Graf ER, et al., Neurexins induce differentiation of GABA and glutamate postsynaptic specializations via neuroligins. Cell, 2004. 119(7): p. 1013–26. [PubMed: 15620359]
33. Ichtchenko K, Nguyen T, and Sudhof TC, Structures, alternative splicing, and neurexin binding of multiple neuroligins. J Biol Chem, 1996. 271(5): p. 2676–82. [PubMed: 8576240]
34. Krueger DD, et al., The role of neurexins and neuroligins in the formation, maturation, and function of vertebrate synapses. Curr Opin Neurobiol, 2012. 22(3): p. 412–22. [PubMed: 22424845]
35. Scheiffele P, et al., Neuroligin expressed in nonneuronal cells triggers presynaptic development in contacting axons. Cell, 2000. 101(6): p. 657–69. [PubMed: 10892652]
36. Sudhof TC, Neuroligins and neurexins link synaptic function to cognitive disease. Nature, 2008. 455(7215): p. 903–11. [PubMed: 18923512]
37. Varoqueaux F, et al., Neuroligins determine synapse maturation and function. Neuron, 2006. 51(6): p. 741–54. [PubMed: 16982420]
38. Baig DN, Yanagawa T, and Tabuchi K, Distortion of the normal function of synaptic cell adhesion molecules by genetic variants as a risk for autism spectrum disorders. Brain Res Bull, 2017. 129: p. 82–90. [PubMed: 27743928]
39. Szatmari P, et al., Mapping autism risk loci using genetic linkage and chromosomal rearrangements. Nat Genet, 2007. 39(3): p. 319–28. [PubMed: 17322880]
40. Taylor SC, et al., The Role of Synaptic Cell Adhesion Molecules and Associated Scaffolding Proteins in Social Affiliative Behaviors. Biol Psychiatry, 2020.
41. Hoon M, et al., Neuroligin-4 is localized to glycinergic postsynapses and regulates inhibition in the retina. Proc Natl Acad Sci U S A, 2011. 108(7): p. 3053–8. [PubMed: 21282647]
42. Song JY, et al., Neuroligin 1 is a postsynaptic cell-adhesion molecule of excitatory synapses. Proc Natl Acad Sci U S A, 1999. 96(3): p. 1100–5. [PubMed: 9927700]
43. Varoqueaux F, Jamain S, and Brose N, Neuroligin 2 is exclusively localized to inhibitory synapses. Eur J Cell Biol, 2004. 83(9): p. 449–56. [PubMed: 15540461]

44. Boucard AA, et al., A splice code for trans-synaptic cell adhesion mediated by binding of neuroligin 1 to alpha- and beta-neurexins. Neuron, 2005. 48(2): p. 229–36. [PubMed: 16242404]
45. Chih B, Engelman H, and Scheiffele P, Control of excitatory and inhibitory synapse formation by neuroligins. Science, 2005. 307(5713): p. 1324–8. [PubMed: 15681343]
46. Dahlhaus R, et al., Overexpression of the cell adhesion protein neuroligin-1 induces learning deficits and impairs synaptic plasticity by altering the ratio of excitation to inhibition in the hippocampus. Hippocampus, 2010. 20(2): p. 305–22. [PubMed: 19437420]
47. Hines RM, et al., Synaptic imbalance, stereotypies, and impaired social interactions in mice with altered neuroligin 2 expression. J Neurosci, 2008. 28(24): p. 6055–67. [PubMed: 18550748]
48. Shipman SL, et al., Functional dependence of neuroligin on a new non-PDZ intracellular domain. Nat Neurosci, 2011. 14(6): p. 718–26. [PubMed: 21532576]
49. Laumonnier F, et al., X-linked mental retardation and autism are associated with a mutation in the NLGN4 gene, a member of the neuroligin family. Am J Hum Genet, 2004. 74(3): p. 552–7. [PubMed: 14963808]
50. Shipman SL and Nicoll RA, Dimerization of postsynaptic neuroligin drives synaptic assembly via transsynaptic clustering of neurexin. Proc Natl Acad Sci U S A, 2012. 109(47): p. 19432–7. [PubMed: 23129658]
51. Kwon HB, et al., Neuroligin-1-dependent competition regulates cortical synaptogenesis and synapse number. Nat Neurosci, 2012. 15(12): p. 1667–74. [PubMed: 23143522]
52. Connor SA, et al., Pumping the brakes: suppression of synapse development by MDGA-neuroligin interactions. Curr Opin Neurobiol, 2019. 57: p. 71–80. [PubMed: 30771697]
53. Connor SA, et al., Altered Cortical Dynamics and Cognitive Function upon Haploinsufficiency of the Autism-Linked Excitatory Synaptic Suppressor MDGA2. Neuron, 2016. 91(5): p. 1052–1068. [PubMed: 27608760]
54. Elegheert J, et al., Structural Mechanism for Modulation of Synaptic Neuroligin-Neurexin Signaling by MDGA Proteins. Neuron, 2017. 96(1): p. 242–244. [PubMed: 28957672]
55. Gangwar SP, et al., Molecular Mechanism of MDGA1: Regulation of Neuroligin 2:Neurexin Trans-synaptic Bridges. Neuron, 2017. 94(6): p. 1132–1141 e4. [PubMed: 28641112]
56. Kim JA, et al., Structural Insights into Modulation of Neurexin-Neuroligin Trans-synaptic Adhesion by MDGA1/Neuroligin-2 Complex. Neuron, 2017. 94(6): p. 1121–1131 e6. [PubMed: 28641111]
57. Lee K, et al., MDGAs interact selectively with neuroligin-2 but not other neuroligins to regulate inhibitory synapse development. Proc Natl Acad Sci U S A, 2013. 110(1): p. 336–41. [PubMed: 23248271]
58. Pettem KL, et al., Interaction between autism-linked MDGAs and neuroligins suppresses inhibitory synapse development. J Cell Biol, 2013. 200(3): p. 321–36. [PubMed: 23358245]
59. Levinson JN, et al., Neuroligins mediate excitatory and inhibitory synapse formation: involvement of PSD-95 and neurexin-1beta in neuroligin-induced synaptic specificity. J Biol Chem, 2005. 280(17): p. 17312–9. [PubMed: 15723836]
60. Stevens HE, et al., Prenatal stress delays inhibitory neuron progenitor migration in the developing neocortex. Psychoneuroendocrinology, 2013. 38(4): p. 509–21. [PubMed: 22910687]
61. Tamamaki N, et al., Green fluorescent protein expression and colocalization with calretinin, parvalbumin, and somatostatin in the GAD67-GFP knock-in mouse. J Comp Neurol, 2003. 467(1): p. 60–79. [PubMed: 14574680]
62. Gorski JA, et al., Cortical excitatory neurons and glia, but not GABAergic neurons, are produced in the Emx1-expressing lineage. J Neurosci, 2002. 22(15): p. 6309–14. [PubMed: 12151506]
63. Phillips GR, et al., Gamma-protocadherins are targeted to subsets of synapses and intracellular organelles in neurons. J Neurosci, 2003. 23(12): p. 5096–104. [PubMed: 12832533]
64. Schoch H, et al., Sociability Deficits and Altered Amygdala Circuits in Mice Lacking Pcdh10, an Autism Associated Gene. Biol Psychiatry, 2017. 81(3): p. 193–202. [PubMed: 27567313]
65. Gao R and Penzes P, Common mechanisms of excitatory and inhibitory imbalance in schizophrenia and autism spectrum disorders. Curr Mol Med, 2015. 15(2): p. 146–67. [PubMed: 25732149]

66. Sohal VS and Rubenstein JLR, Excitation-inhibition balance as a framework for investigating mechanisms in neuropsychiatric disorders. Mol Psychiatry, 2019. 24(9): p. 1248–1257. [PubMed: 31089192]

67. Sun C, et al., Identification and functional characterization of rare mutations of the neuroligin-2 gene (NLGN2) associated with schizophrenia. Hum Mol Genet, 2011. 20(15): p. 3042–51. [PubMed: 21551456]

68. Fabrichny IP, et al., Structural analysis of the synaptic protein neuroligin and its beta-neurexin complex: determinants for folding and cell adhesion. Neuron, 2007. 56(6): p. 979–91. [PubMed: 18093521]

69. Rubinstein R, et al., Structural origins of clustered protocadherin-mediated neuronal barcoding. Semin Cell Dev Biol, 2017. 69: p. 140–150. [PubMed: 28743640]

70. Brasch J, et al., Visualization of clustered protocadherin neuronal self-recognition complexes. Nature, 2019. 569(7755): p. 280–283. [PubMed: 30971825]

71. Chanda S, et al., Unique versus Redundant Functions of Neuroligin Genes in Shaping Excitatory and Inhibitory Synapse Properties. J Neurosci, 2017. 37(29): p. 6816–6836. [PubMed: 28607166]

72. Lim J, et al., Autism-like behaviors in male mice with a Pcdh19 deletion. Mol Brain, 2019. 12(1): p. 95. [PubMed: 31747920]

73. Katayama Y, et al., CHD8 haploinsufficiency results in autistic-like phenotypes in mice. Nature, 2016. 537(7622): p. 675–679. [PubMed: 27602517]

74. Blundell J, et al., Increased anxiety-like behavior in mice lacking the inhibitory synapse cell adhesion molecule neuroligin 2. Genes Brain Behav, 2009. 8(1): p. 114–26. [PubMed: 19016888]

75. Gkogkas CG, et al., Autism-related deficits via dysregulated eIF4E-dependent translational control. Nature, 2013. 493(7432): p. 371–7. [PubMed: 23172145]

76. Liang J, et al., Conditional knockout of Nlgn2 in the adult medial prefrontal cortex (mPFC) induces delayed loss of inhibitory synapses. Mol Psychiatry, 2015. 20(7): p. 793. [PubMed: 26098222]

77. Wohr M, et al., Developmental delays and reduced pup ultrasonic vocalizations but normal sociability in mice lacking the postsynaptic cell adhesion protein neuroligin2. Behav Brain Res, 2013. 251: p. 50–64. [PubMed: 22820233]

78. Biederer T and Scheiffele P, Mixed-culture assays for analyzing neuronal synapse formation. Nat Protoc, 2007. 2(3): p. 670–6. [PubMed: 17406629]

79. Brodkin ES, et al., Social approach-avoidance behavior of inbred mouse strains towards DBA/2 mice. Brain Res, 2004. 1002(1–2): p. 151–7. [PubMed: 14988045]

80. Fairless AH, et al., Deconstructing sociability, an autism-relevant phenotype, in mouse models. Anat Rec (Hoboken), 2011. 294(10): p. 1713–25. [PubMed: 21905241]

81. Sankoorikal GM, et al., A mouse model system for genetic analysis of sociability: C57BL/6J versus BALB/cJ inbred mouse strains. Biol Psychiatry, 2006. 59(5): p. 415–23. [PubMed: 16199013]

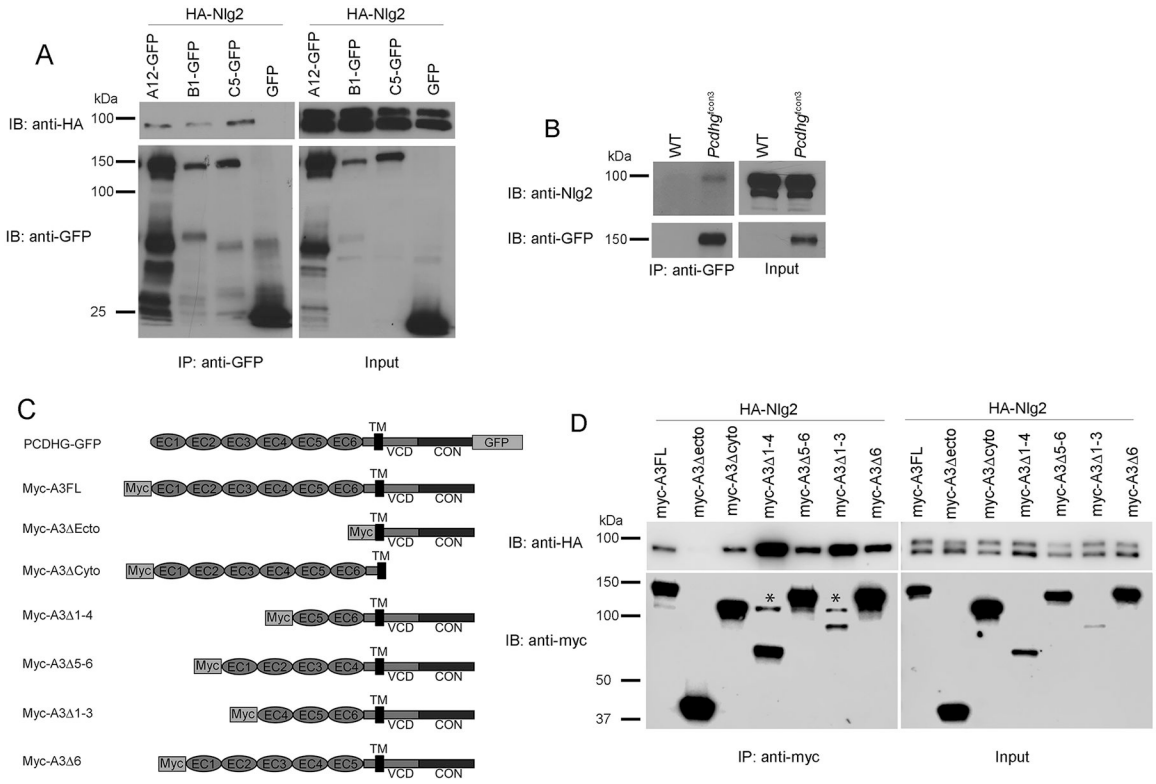

Figure 1. Multiple γ-Pcdhs interact with Neuroligin-2 *in vitro* and *in vivo*.

(A) In co-transfected COS cells, N-terminally-tagged Nlg2 co-immunoprecipitates with multiple full-length γ-Pcdhs C-terminally tagged with GFP, but not with a GFP-only control. (B) Using GFP-Trap nanobodies, endogenous Nlg2 co-immunoprecipitates with γ-Pcdhs in cortical lysates from *Pcdhg*$^{fcon3/fcon3}$ mice, in which all 22 γ-Pcdhs are C-terminally GFP-tagged (see also panel C). No such co-immunoprecipitation is seen in lysates from wild-type mice. (C) Schematic representation of the various full length and truncated γ-Pcdh construct protein structures utilized for co-immunoprecipitation. Full length γ-Pcdhs consist of 6 extracellular cadherin (EC) domains, a single transmembrane domain (TM), and a cytoplasmic portion containing both a variable domain (VCD) and a shared constant domain (CON). (D) In co-transfected COS cells, HA-Nlg2 co-immunoprecipitates with full-length γ-Pcdh-A3, A3 lacking the cytoplasmic domain (Δcyto), and (to differing extents) A3 lacking some of the EC repeats; co-immunoprecipitation is completely lost only with constructs lacking all 6 EC domains (Δecto). Asterisks denote residual HA-Nlg2 band signal after the blot was stripped and re-probed for myc.

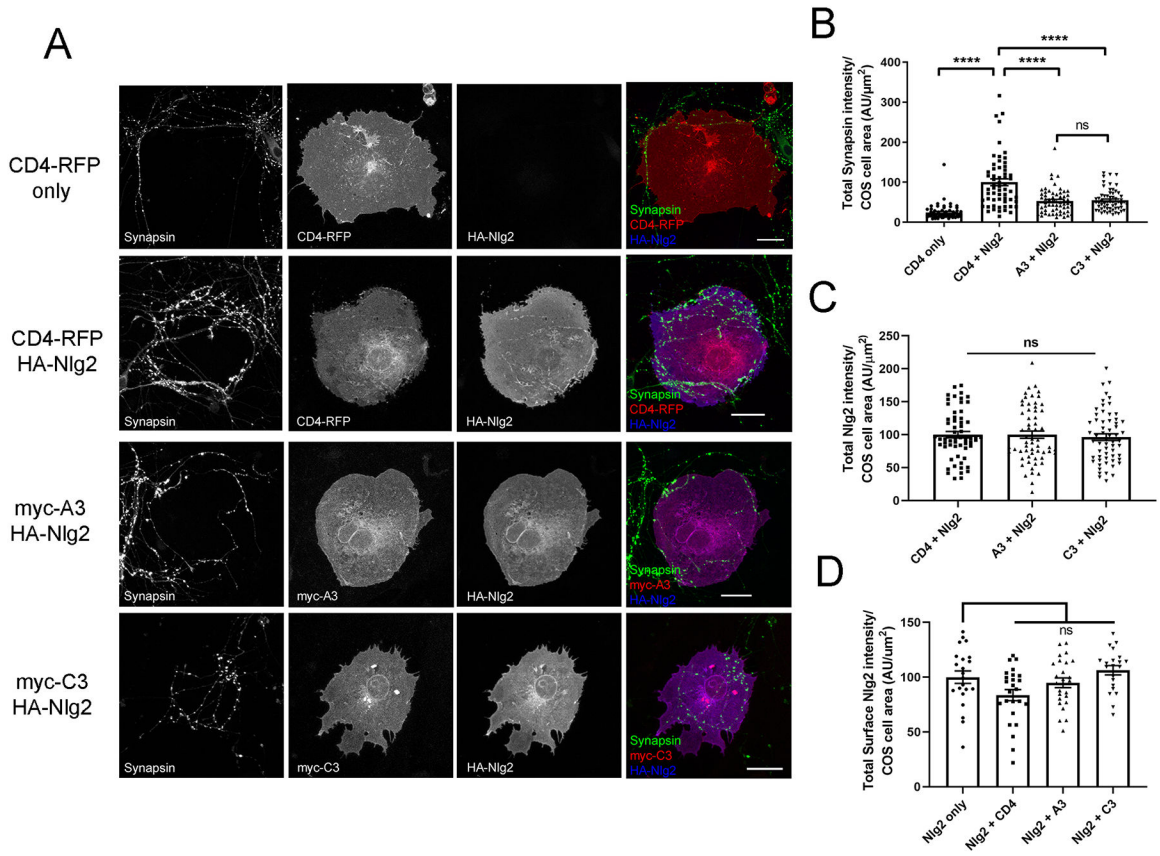

Figure 2. γ-Pcdhs reduce the synaptogenic activity of Nlg2 in the artificial synapse assay.

(A) COS cells were co-transfected with HA-Nlg2 and either a control construct (CD4-RFP), or a myc-tagged γ-Pcdh-A3 or γ-Pcdh-C3 construct (myc-A3 or myc-C3), and subsequently co-cultured with hippocampal neurons. Cells expressing CD4-RFP alone exhibited little presynaptic differentiation in contacting axons, calculated as synapsin intensity over COS cell area (B). As demonstrated in many prior studies, COS cells expressing Nlg2 (along with the inert CD4) exhibited robust pre-synaptic differentiation in contacting axons. However, when COS cells co-expressed Nlg2 and either γ-Pcdh construct, there was a significant decrease in synapsin clustering, indicating that γ-Pcdhs can negatively regulate Nlg2's ability to promote presynaptic differentiation *in vitro*. There were no significant changes in either overall Nlg2 expression (C), nor in Nlg2 surface expression (D) in COS cells co-expressing control *vs.* γ-Pcdh constructs. Data are presented as mean ± SEM, normalized as % of control to CD4-Nlg2 (B, C) or Nlg2 only (D); dots indicate individual COS cells analyzed. n=60 cells per condition for 2B and 2C, n=21–25 cells per condition for 2D. One-way ANOVA, Tukey's multiple comparison test, *p<0.05, **p<0.01, p***<0.001, p****<0.0001. AU=arbitrary units. Scale bar, 20 μm.

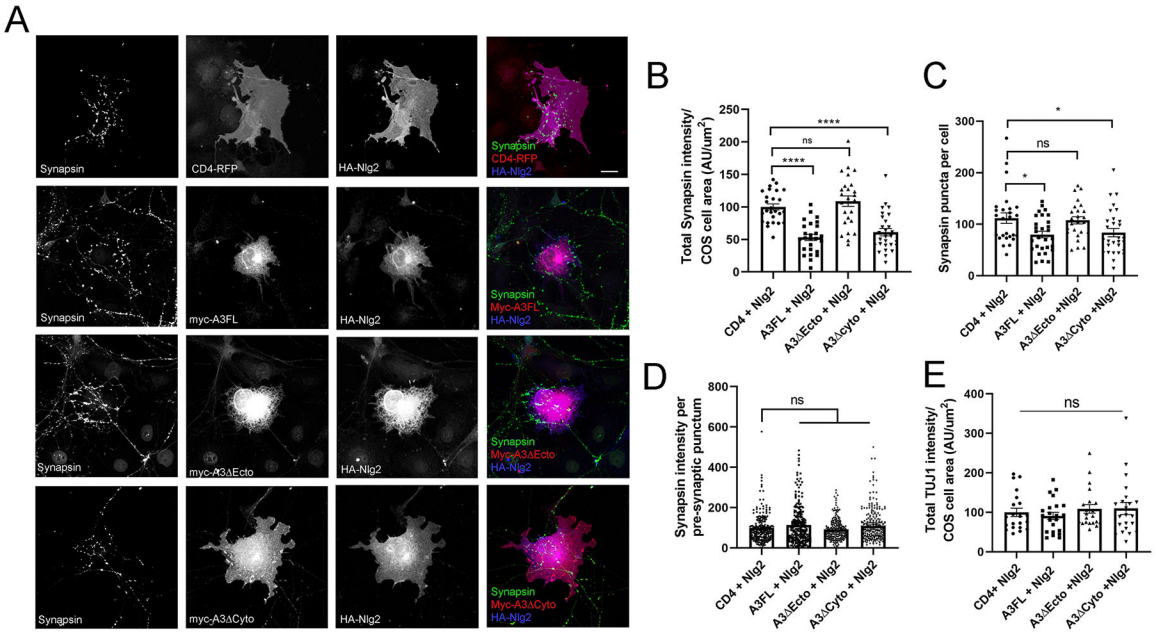

Figure 3. The γ-Pcdh extracellular domain is necessary for inhibition of Nlg2 function in the artificial synapse assay.

COS Cells were co-transfected with HA-Nlg2, and either myc-A3FL, myc-A3ΔEcto, myc-A3ΔCyto, or CD4-RFP. Transfected cells were co-cultured with hippocampal neurons (A). As in other assays (Figure 2), co-expression of A3FL with Nlg2 resulted in reduced synapsin intensity per COS cell area. Similarly, A3ΔCyto significantly reduced Nlg2 induction of presynaptic differentiation in contacting axons; A3ΔEcto, however had no such effect (B), consistent with co-immunoprecipitation results indicating an extracellular interaction with Nlg2. Re-analysis of these experiments to quantify the number of synapsin puncta per cell (C) and the fluorescence intensity of individual synapsin puncta (D) was performed. This showed that the former tracked the results in (B) while the latter did not change across transfection conditions; thus γ-Pcdhs, via their ectodomains, reduce the number, but not intensity, of synapsin puncta induced in contacting axons by Nlg2. To ensure that differences seen between conditions were not attributable to effects on neurite outgrowth over the COS cells, the intensity of TUJ1 immunoreactivity was measured (E). No significant difference was seen across conditions. n= 25–30 COS cells per condition. Data are presented as mean ± SEM, normalized as % of control (CD4 + Nlg2); dots indicate individual COS cells analyzed. One-way ANOVA, Tukey's multiple comparisons test *p<0.05, **p<0.01, p***<0.001, p****<0.0001. Scale Bar, 20 μm.

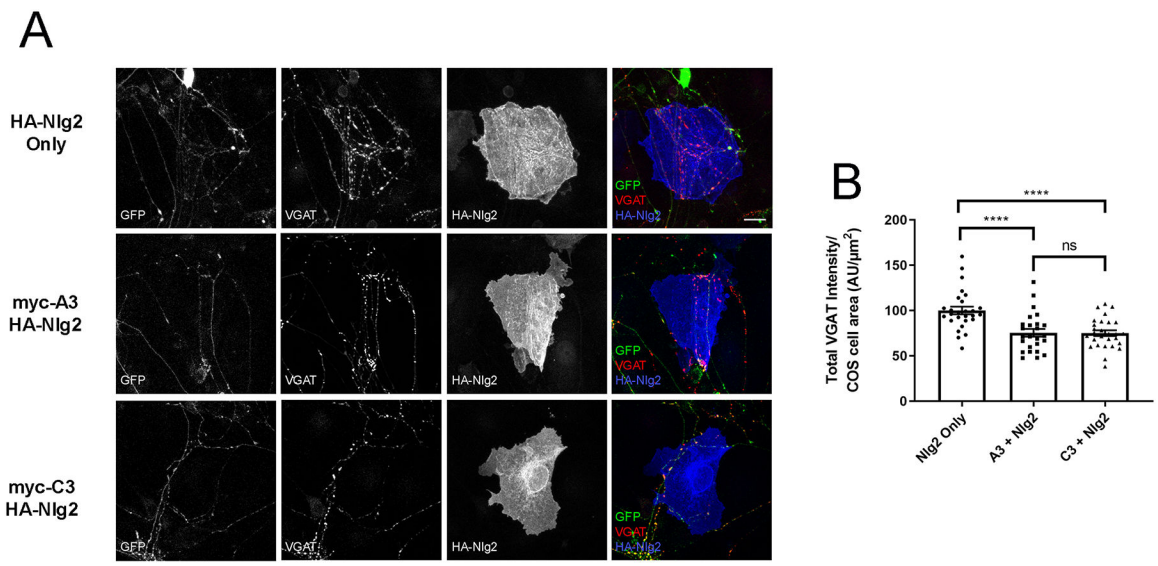

Figure 4. γ-Pcdhs reduce the ability of Nlg2 to recruit VGAT in inhibitory axons in the artificial synapse assay.

COS cells were transfected with HA-Nlg2, or HA-Nlg2 and a myc-tagged γ-Pcdh construct (myc-A3 or myc-C3) and co-cultured with hippocampal neurons taken from *Gad67-GFP* mice in which inhibitory interneuron processes are GFP labeled. Pre-synaptic differentiation specific to these inhibitory axons was calculated as VGAT intensity over COS cell area (B). Similarly to the assays shown in Figure 2, COS cells expressing both Nlg2 and either γ-Pcdh construct exhibited a significant decrease in inhibitory presynaptic differentiation of contacting axons as compared to COS cells expressing Nlg2 alone. These data indicate that γ-Pcdhs can negatively regulate inhibitory presynaptic differentiation mediated through Nlg2 *in vitro.* n= 25–28 per condition. Data are presented as mean ± SEM, normalized as % of control to Nlg2 only (B); dots indicate individual COS cells analyzed. One-way ANOVA, Tukey's multiple comparisons test *p<0.05, **p<0.01, p***<0.001, p****<0.0001. Scale bar, 20 μm.

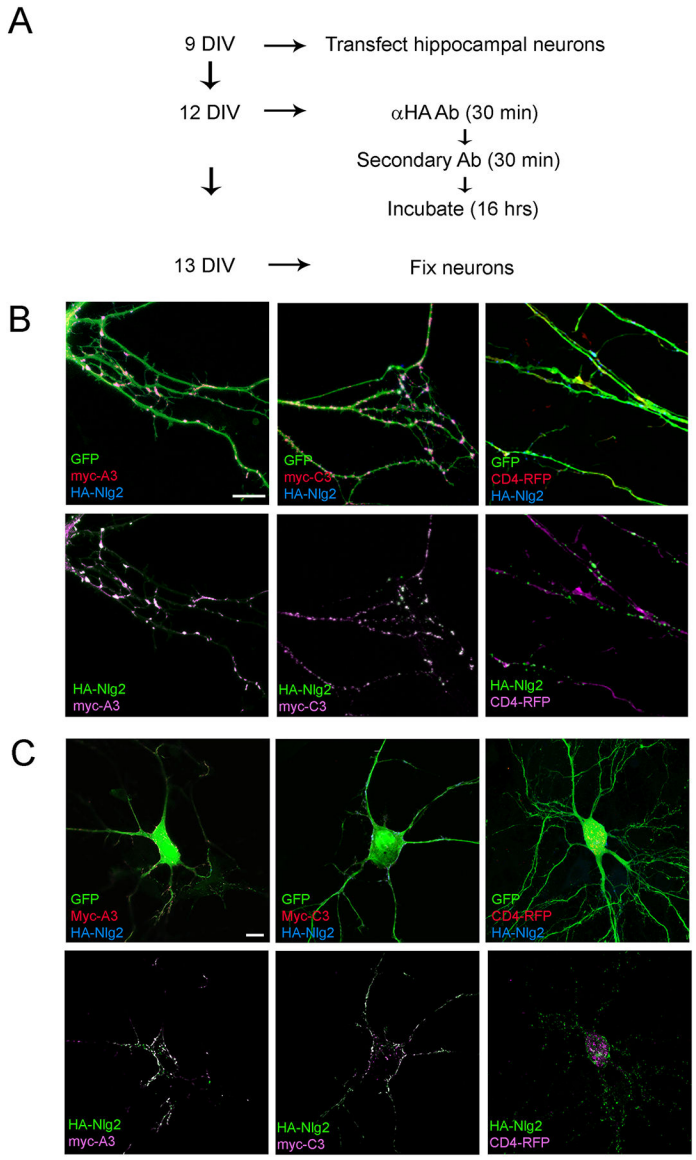

Figure 5. γ-Pcdhs can co-aggregate *in cis* with Nlg2 on the neuronal cell surface.

Hippocampal neurons were transfected after 9 days *in vitro* (DIV) with constructs encoding GFP, HA-Nlg2, and either a myc-γ-Pcdh construct (A3 or C3), or a control construct (CD4-RFP). Live neurons were then incubated with rat anti-HA antibodies followed by Alexa 647-conjugated goat anti-rat secondary antibodies to artificially induce surface aggregation of HA-Nlg2 into patches on the neuronal cell surface. After an additional 16 hours of incubation, cultures were fixed, stained, and imaged (A; experimental workflow). Both A3 and C3 were found to co-aggregate with Nlg2 at the dendritic cell surface, while no significant co-aggregation was seen when neurons were transfected with HA-Nlg2 and CD4-RFP (control) (B). Similarly, both γ-Pcdhs (but not CD4-RFP) co-localized with Nlg2 at the cell body surface (C). Scale bar, 15 μm.

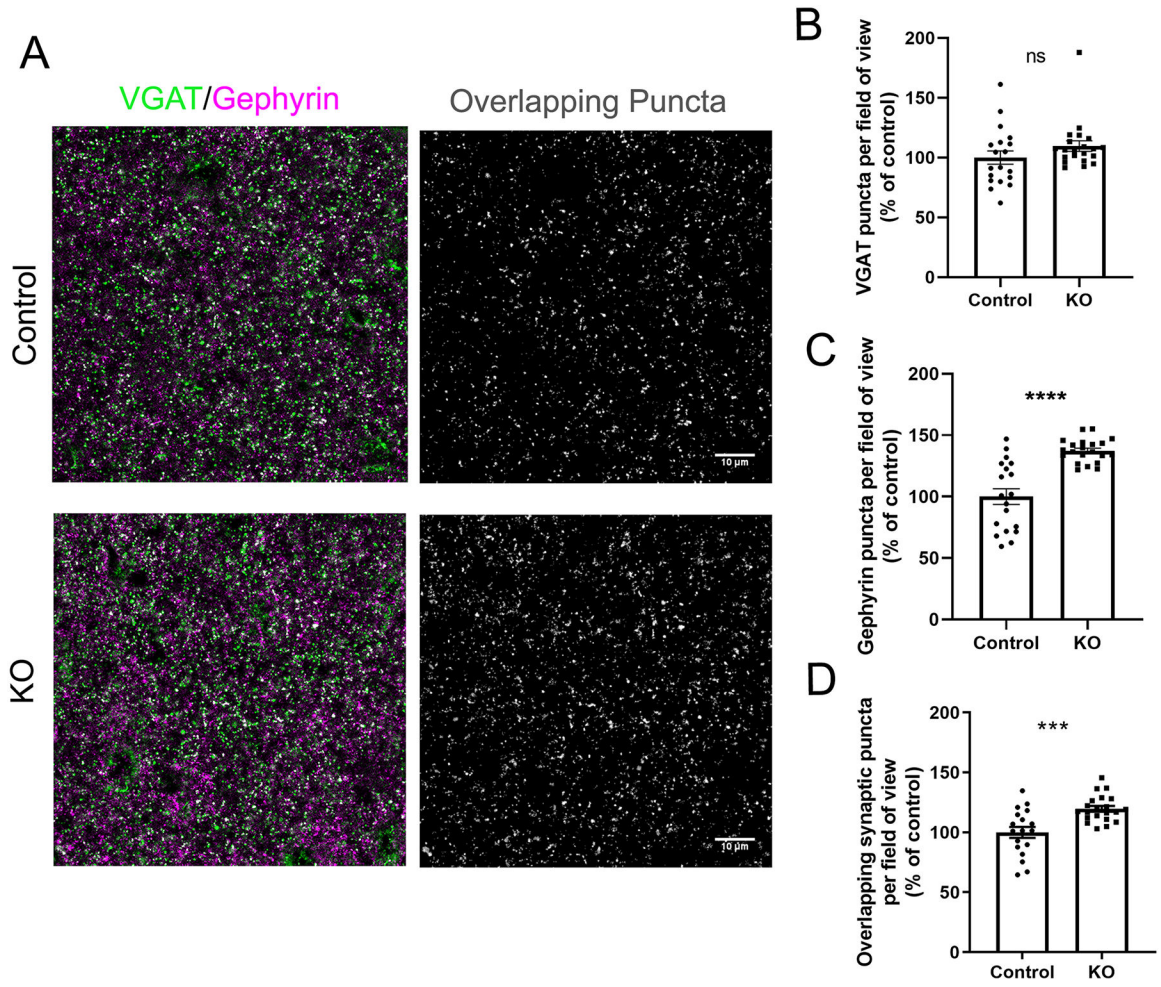

Figure 6. *Pcdhg* mutant mice exhibit increased density of inhibitory synaptic puncta in the cortex.

Primary somatosensory cortices of control (*Pcdhg*$^{fcon3/fcon3}$) and experimental (*Emx1-Cre;Pcdhg*$^{fcon3/fcon3}$; KO) mice were cryosectioned and stained with antibodies against VGAT (green) and gephyrin (magenta) to label inhibitory pre- and post-synaptic localizations, respectively (A). Inhibitory synapse density was estimated by extracting and counting the number of co-localized pre- and post-synaptic puncta per field of view (shown in white). When excitatory neurons postsynaptic to inhibitory interneurons lacked all γ-Pcdhs, density of VGAT puncta was not significantly altered (B), while both gephyrin (C) and overlapping synaptic puncta (D) were significantly increased. n=18 (control) or 21 (KO) fields of view. Data are presented as mean ± SEM; dots indicate individual fields of view. Unpaired t-test, p***<0.001 p****<0.0001. Scale bar, 10 µm.

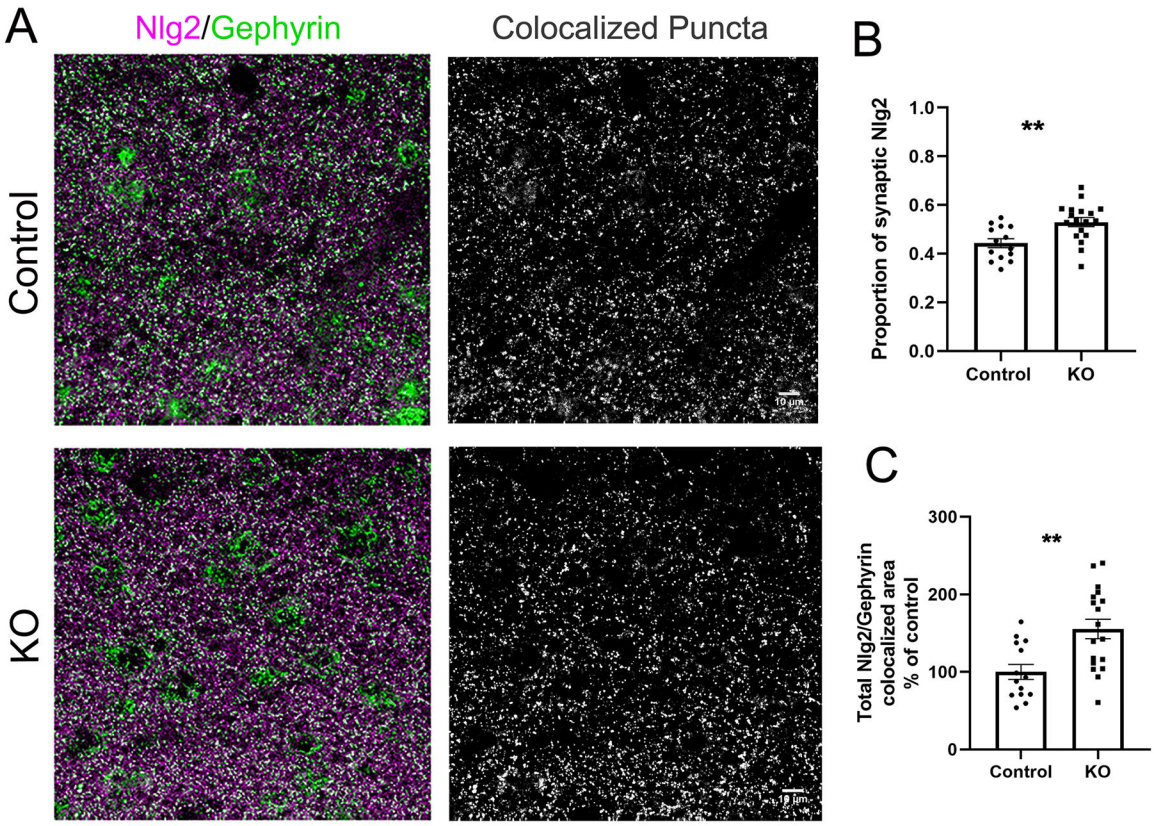

Figure 7. Increased colocalization of Nlg2 with gephyrin in *Pcdhg* mutant cortex.

Primary somatosensory cortices of control (*Pcdhg*$^{fcon3/fcon3}$) and experimental (*Emx1-Cre;Pcdhg*$^{fcon3/fcon3}$; KO) mice were cryosectioned and stained with antibodies against Nlg2 (magenta) and gephyrin (green; A). Proportion of synaptically-localized Nlg2 puncta was calculated by quantifying the number of colocalized Nlg2+/gephyrin+ puncta (white) and dividing by total number of total Nlg2 puncta (B). This proportion is significantly increased in *Pcdhg* mutant cortex, as is total Nlg2+/gephyrin+ post-synaptic area (C). n=14 (control) or 18 (KO) fields of view, Data are presented as mean ± SEM; dots indicate individual fields of view. Unpaired t-test, p**<0.01. Scale bar, 10 µm.

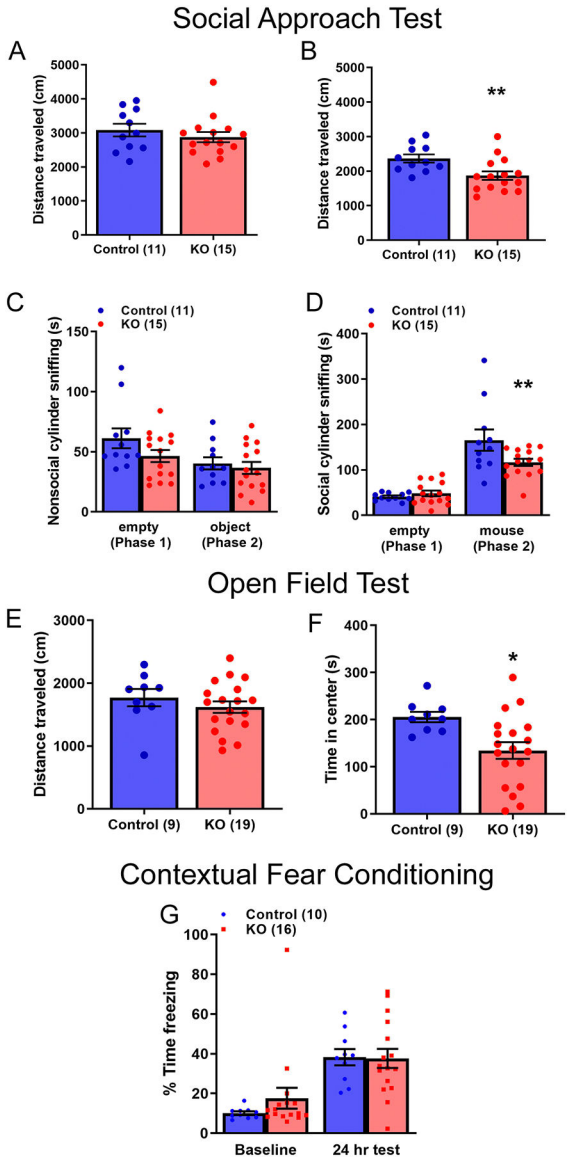

Figure 8. Mice lacking γ-Pcdhs in the dorsal forebrain exhibit behavioral deficits in social approach and open field tests.

Control (*Emx1-Cre;Pcdhg*$^{fcon3/+}$) and dorsal forebrain knockout (*Emx1-Cre;Pcdhg*$^{fcon3/fcon3}$; KO) mice were analyzed in the indicated behavioral tests (see Methods for details). (A) KO mice travel a similar distance as their control littermates during habituation in Phase 1 of the 3-chamber social approach test. (B) In Phase 2, when the novel object and social stimulus are present, KO mice travel less than control littermates. (C) KO and control littermates spend similar amounts of time sniffing the nonsocial cylinder in Phase 1 when the cylinder is empty and in Phase 2 when it contained a novel object. (D) However, KO mice spend less time sniffing the social cylinder than control littermates in Phase 2 when the cylinder contained a novel social stimulus. **p<0.01. (E) In the open field test, KO mice travel a similar distance as their control littermates. However, KO mice spend less time in the center of the open field than do control littermates (F), indicating anxiety-

like behavior. *p<0.05. (G) KO and control littermate mice spend a similar percentage of time freezing at baseline and during the 24-hour test in a contextual fear conditioning text.